

# Artificial Neural Network- Genetic Algorithm based Optimization of Baffle Assisted Jet Array Impingement Cooling with Cross-Flow

S. Kurian<sup>1†</sup>, J. Johnson<sup>2</sup>, P. S .Tide <sup>1</sup> and N. Biju<sup>1</sup>

<sup>1</sup> *Cochin University of Science and Technology, Cochin, Kerala, India*

<sup>2</sup> *Mar Athanasius College of Engineering, Kothamangalam, Kerala*

†*Corresponding Author Email: sabukurian74@gmail.com*

(Received May 22, 2021, accepted October 4, 2021)

## ABSTRACT

The objective of this research is to numerically investigate heat transfer and pressure drop characteristic of a baffle assisted multi-jet impingement of air on a heated plate subjected to constant heat flux and cross flow. Two baffle configurations were considered for the present study. An array of jets with 3 x 3 configurations discharging from round orifices of diameter  $D=5$  mm and with jet-to-heated plate distance ranging from  $2D$  to  $3.5D$  were studied. SST  $k-\omega$  turbulence model was used for numerical simulation to examine the effect of blow ratio and baffle clearance on heat transfer and pressure drop characteristics. Blow ratios of 0.25, 0.5, 0.75 and 1.0 and baffle clearances of 1 mm, 2 mm, and 3mm were considered for CFD simulations. The split baffle configuration with baffle clearance of 3 mm is found to be more advantageous when both heat transfer and pressure drop are considered. However, the segmented baffle configuration with a baffle clearance of 1 mm gave better results for heat transfer alone. The present study also deals with determination of optimal operating parameters with the help of Genetic Algorithm and Artificial Neural Network. A pareto front was obtained for selecting the desired value of heat transfer or pressure drop. It was found that Artificial Neural Network based predictions strongly agree with CFD simulation results, and hence seems to be very useful in arriving at the optimum values of operating parameters.

**Keywords:** Jet impingement; Baffles; Blow ratio; Artificial Neural Network; Genetic algorithm.

## NOMENCLATURE

$BR$	blow ratio	$Nu_0$	Nusselt number without baffles
$C$	baffle clearance	$f$	friction factor
$D$	jet diameter	$f_0$	friction factor without baffles
$h$	heat transfer coefficient	$V_c$	cross flow velocity
$H$	nozzle to plate distance	$x$	length along stream wise direction
$Nu$	Nusselt number	$\phi$	thermo-hydraulic performance

## 1. INTRODUCTION

Considerable emphasis was given by the engineering community to meet the ever-growing heat transfer requirements for modern thermal systems. Heat transfer augmentation is an important topic of research in the field of thermal engineering. Jet impingement is one of the best and proven heat transfer enhancement processes among the different single-phase convective heat transfer techniques. Relatively high heat transfer rates with moderate pressure drop are the distinct advantages of jet impingement systems. Impinging jets has a lot of

industrial applications such as drying of food products and papers, annealing of plastic, shaping and tempering of glass, and sheet metals, electronics thermal management and anti-icing of aircraft wings etc. A schematic of flow field development in a single impinging jet is shown in Fig. 1. The free jet emanated out of the nozzle, consists of a potential core and a shear layer. In the potential core, the velocity of flow remains nearly same as that of the jet velocity at nozzle exit. A shear layer is formed at the boundary of potential core because of the entrainment of surrounding fluid. In the vicinity of nozzle, the shear layer is thin and its thickness

increases towards the downstream. Flow from a nozzle can be laminar or turbulent depending on the Reynolds number. Turbulent transition of the laminar flow begins at the shear layer which is unstable and causes roll-up of vortices. These vortices are transported downstream along with jet flow causes more and more entrainment. Later these vortices grow, pair, lose symmetry and eventually break up into eddies and finally flow becomes fully developed. A stagnation zone is formed near the target plate characterized by a pressure gradient, which causes discontinuity of the flow in the axial direction, and flow turns into the radial direction. The impinging jet that spreads radially in all directions along the target surface is called a wall jet.

Various mechanisms of convective heat transport and possible applications for impinging jets were reported by [Jambunathan \*et al.\* \(1992\)](#) and [Zukerman \*et al.\* \(2006\)](#). Heat transfer and fluid flow distribution of single impinging jets have been performed experimentally and numerically, and reported in numerous literatures such as [Van Heiningen \*et al.\* \(1976\)](#), [Chen \*et al.\* \(2000\)](#) and [Lou \*et al.\* \(2005\)](#).

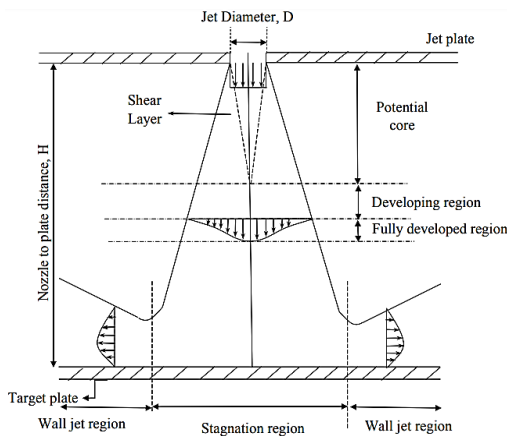


**Fig. 1. Flow field of a simple jet impingement system.**

[Metzger and Korstad \(1972\)](#) studied the effect of cross-flow on a single line of jets, emanating from circular orifice. They found that jet Reynolds number,  $H/D$ , and the cross-flow influences heat transfer on the target wall. [Chance \(1974\)](#) investigated the influence of jet-to-target-plate distance considering low-speed jets with cross flow in one direction. Variations in cross flow velocities and static pressure were observed with decrease in jet to heated plate distance. [Metzger \*et al.\* \(1979\)](#) pointed out that in-line pattern provides better heat transfer than staggered pattern of an array of impinging jets, for low-speed situations. [Florschuetz \*et al.\* \(1981\)](#) developed a correlation for Nusselt number dependence on flow pattern, Reynolds number, Prandtl number and jet impingement plate geometry for an in-line and staggered jet patterns, with cross flow exits in one direction. [Obot and Trabold \(1987\)](#) investigated the effects of jet-to-target-plate distance in low Reynolds number. It was observed that for a given scheme of cross-flow and

jet diameter  $D$ , higher coefficient of heat transfer was obtained as the number of jets increased over a fixed target area. [Wang \*et al.\* \(2005\)](#) explored the heat transfer characteristics for an in-line pattern jet array. In their work, deterioration of the heat transfer characteristics was noticed with increasing cross-flow velocity. Heat transfer characteristics of jet arrays were investigated by [Mohamed \(2006\)](#) with multiple components kept in a passage of adjustable height. An increase in the average heat transfer coefficient was noticed with increasing component to passage height ratio. [Yemenici \*et al.\* \(2012\)](#) investigated the air-cooling characteristics in arrays of rectangular protrusions immersed in a boundary layer. It was concluded that, augmenting the height of the protrusions intensify the heat transfer, particularly when the boundary layer is in laminar regime.

In electronics cooling, cross-flow cooling strategy lacks flexibility due to the differential heat dissipation demand of components in printed circuit boards. In such cases, cooling requirement of hot-spots determine the quantity of circulating air. This result in a higher mass flow rate and increased pressure drop, which in turn increases the fan power. In order to overcome this defect, a combination of high velocity jet impingement with a low-velocity cross-flow scheme was proposed by different researchers. The impinging air jets are kept over the high heat generating component and produce local regions of higher heat transfer. Meanwhile, cross-flow provides uniform cooling performance, where lower heat dissipation is required. Jet impingement in a cross-flow was experimentally studied by [Tummers \*et al.\* \(2005\)](#) and [Masip \*et al.\* \(2012\)](#), and numerically by [Popovac and Hanjalic \(2007, 2009\)](#) and by [Rundström and Moshfegh \(2006, 2008\)](#). [Tummers \*et al.\* \(2005\)](#) studied the flow dynamics around the hot component, as a result of the synergy between the impinging jet and cross-flow. Furthermore, local temperature variations were linked with flow behavior and studied the consequence of jet shift on the total heat transfer.

There had been a number of attempts to complement jet impingement with other heat transfer enhancing techniques such as ribs, baffles, vortex generators and tape twistors etc. These modifications alter the flow field to enhance the turbulence and mixing of fluid mediums that cause increased cooling performance. Experimental and numerical investigations were conducted by [Yu \*et al.\* \(2016\)](#) on multiple jet impingements over W-shaped micro-rib structure attached test plates under maximum cross flow conditions. Appreciable increase in area averaged heat transfer rate for ribbed plates was noticed in their study. [Dhanasegaran and Pugazhendhi \(2017\)](#) studied the flow dynamics and heat transfer characteristics of a jet emanating from a corrugated orifice plate on a heated plate. Anti-cross flow was noticed and related effects such as up-wash fountain and wall eddies were observed. Unlike corrugations and swirls, baffles are discrete objects which can create localized and intense disturbances in the flow field. Use of baffles may have exorbitant effects in the case of jet impingement cooling with

cross flow. [Berner \*et al.\* \(1984\)](#) noticed the specific features of the flow through baffles and visualized extra turbulence created in the flow. Baffle spacing together with overlap and velocity of flow were the factors that they considered. The baffle plate creates better mixing, causes better turbulence and hence higher heat transfer.

Pressure drop created by the baffles are enormous. Baffles are to be designed based on the acceptable pressure drop in the system. [Habib \*et al.\* \(1992\)](#) and [Dutta \*et al.\* \(1997\)](#) explored the heat transfer increment with an inclined perforated baffle. It was observed that studies pertaining to combination of impinging jets with insertion of baffles are rare in the literature.

Various studies were observed with multiple turbulence models to determine accuracy of the results in comparison with the experimental results of similar flow domain. In their numerical study of turbulent circular impinging jets, [Craft \*et al.\* \(1996\)](#) tested four turbulence models, which include one  $k-\epsilon$  eddy viscosity model and three second-moment closures. Nature of flow field in the region of the stagnation zone was investigated by [Angioletti \*et al.\* \(2003\)](#). By comparing the experimental and numerical findings, they estimated the robustness of three types of turbulence models with the help of CFD tools. Later they concluded that, for lower Reynolds number, the SST  $k-\omega$  model gave best results, while for higher Reynolds number,  $k-\epsilon$  RNG and RSM model offered superior performance. [Shukla and Dewan \(2017\)](#) reported that standard  $k-\omega$  model and SST  $k-\omega$  model has showed better accuracy compared to variants of  $k-\epsilon$  model for slot jet impingement over flat and ribbed surfaces. For flow through baffles, [Nasiruddin \*et al.\* \(2007\)](#) has studied the four different turbulent models namely Spalart–Allmaras model,  $k-\epsilon$  model,  $k-\omega$  model, and Reynolds stress model. On comparing the simulation results with the experimental data, SST  $k-\omega$  turbulence model was found to be the best to predict the flow modification due to the baffle. According to them, the advantage of this turbulence model is its capacity to calculate rapidly emerging flow, capture behavior on both near wall and far field regions and predict the interactions with the wall.

The dominant factors affecting heat transfer in a multi-jet impingement are well investigated in the above literature. It is observed that an increase in cross-flow due to spent air of jets causes decrease in heat transfer. Therefore, much research is not carried out in the cases of initial cross-flow. However, introduction of baffles into the flow field will certainly alter the flow dynamics caused by the initial cross-flow and heat transfer characteristics of the system.

Recently, a few research works on multi-jet air impingement reported, which employs novel optimization techniques for design of experimental and numerical analysis. [Chandramohan \*et al.\* \(2017\)](#) and [Ilyas \*et al.\* \(2019\)](#) devised a principal

component analysis for optimizing variables such as H/D, Reynolds number and pipe diameter and swirl flow. Analysis of Variance (ANOVA), showed that, H/D ratio and Reynolds number are significantly affected heat transfer characteristics. Another study carried out by [Chandramohan \*et al.\* \(2021\)](#) employed response surface methodology (RSM) for the design of experiments and multi-objective optimization was carried out using desirability analysis to find optimum input parameters.

In the present study, effect of the baffle configuration on heat transfer characteristics of multiple impinging steady air jets with confinement was numerically investigated at different forced cross-flow velocities maintaining constant jet to heated plate distance. Numerical techniques were used to simulate the flow patterns under various conditions by using appropriate turbulence model and the results were validated with experimental measurements obtained for one set of baffle configuration. For the second set of baffle configuration, only numerical simulation was performed. The focus of the investigation was to study effect of baffle clearance and blow ratios for different baffle arrangements in view of increasing the heat transfer characteristics and decreasing the pressure drop.

## 2. EXPERIMENTAL SET-UP

Experimental set-up for the present study consists of jet impingement facility, cross-flow and baffle arrangements, data acquisition system and flow measuring devices. The schematic of test rig is shown in Fig. 2. Atmospheric air is drawn by a 7.5 hp centrifugal blower and heated to a constant temperature of 300 K using an air pre-heater. The measurements showed that ambient air temperature at suction conditions was between 293 to 297 K. A portion of intake air supplied to a plenum chamber fixed with a nozzle plate having 9 nozzles in 3 x 3 in-line array. Two layers of honeycomb meshes were provided in the plenum chamber for attaining uniform flow and ensuring constant velocity of 38 m/s at exit of all nozzles. Cross-flow for the test section was obtained from the remaining fraction of preheated air. Air flow towards the plenum chamber and cross-flow was measured using calibrated orifice meters. A tapered rectangular section duct was provided in order to provide uniform cross-flow normal to jet impingement. A foil type heater with 50 W load was attached at the bottom side of the heated plate of dimension 120 x 120 mm and made of aluminum.

A Y-traverser mechanism was employed to fix the space between the heated plate and the nozzle exit plane. The cross-flow passing through the clearance with high velocity may act as a secondary jet over the heated plate. Temperatures at the eighteen discrete locations of the heated plate are measured with K-type thermocouples, located on the plate surface. Initial cross-flow enters the heated plate from one side and leaves through the other side,

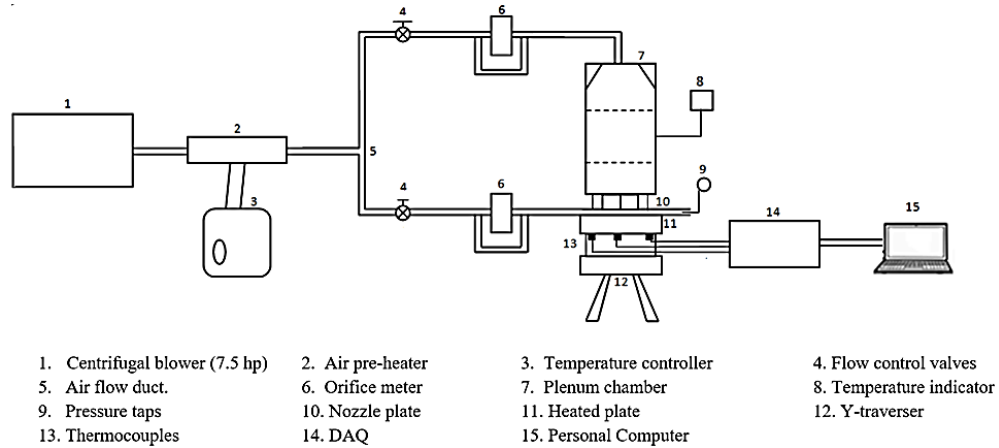


**Fig. 2. Schematic diagram of experimental setup.**

while the span-wise sides are confined. The cross-flow passes through a set of baffles of specific configuration. Clearance is provided between the baffle and heated plate to avoid hot spots. Using an 18-channel data acquisition module (DAQ) and a personal computer, real-time temperatures were recorded. The DAQ, thermocouples, orifice meter, U-tube manometer, temperature controller of air pre-heaters etc. used for measurements were NABL calibrated. Using the method described by Kline and McClintock (1953), uncertainty in jet velocity is estimated to be  $\pm 5.38\%$ .

Experiments were conducted at constant jet velocity and varying the cross-flow velocities so as to have blow ratios of 0.25, 0.50, 0.75, and 1.0. The crossflow strength is represented as blow ratio which is defined as the ratio of cross-flow velocity to jet velocity. Four baffles were placed in the cross-flow passage above the heated plate with clearance of 1 mm, 2 mm and 3 mm. Jet-to-heated plate distance ranging from 2D to 3.5D was considered for this study. Experiments were performed for the validations of the numerical model and it was performed with baffle configuration 1 as shown in Fig. 3. Each baffle has half the length of the heated plate (60 mm) which moderately deflects the cross-flow causing enhanced turbulence. Under identical ambient conditions, experiments were repeated thrice to ensure repeatability of results.

### 3. NUMERICAL APPROACH.

A three-dimensional physical domain consisting of an in-line 3 x 3 array of nozzles, a heated plate of 120 x 120 mm aluminum plate and four layers of baffles was considered for the investigation. Based on arrangement of baffles, two types of baffle configurations were considered for the present study. Configurations 1 and 2 represent segmented and split baffles respectively and the wireframe model of the physical domain for both configurations are represented in Fig. 3.

Cross-flow enters through one side of the domain and leaves through the other side, while the jet enters perpendicular to the cross-flow direction. The other two sides of the domain are confined. Jets are circular

in shape having a diameter  $D = 5$  mm. Discretization of the computational domain was carried out with structured hexahedral mesh. Airflow is assumed to be three-dimensional, incompressible, steady, and viscous. Effects of radiation, gravity, and viscous dissipation were neglected. Specific heat, density, and thermal conductivity of air were assumed to be constant.

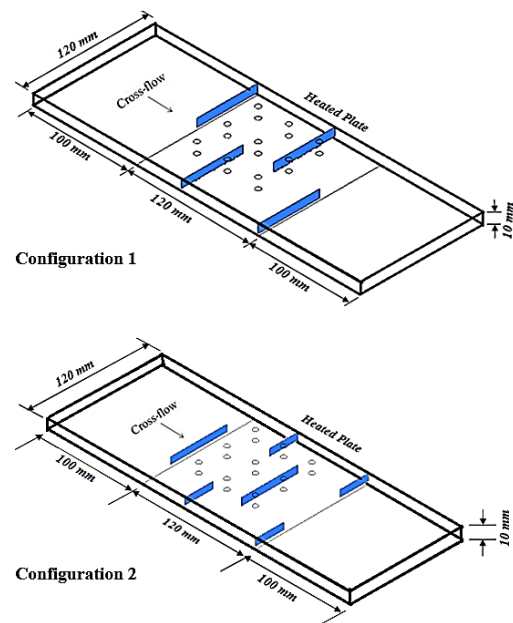


**Fig. 3. Wireframe model of the physical domain for configuration 1 and configuration 2.**

A constant heat flux of  $3472 \text{ W/m}^2$  was supplied to the heated plate. Confinement walls are assumed adiabatic, while nozzle and cross-flow inlets are specified as ‘velocity inlet’ boundary conditions. Jet velocity is a constant at 38 m/s, while cross-flow velocity is made as a variable, determined by the blow ratio considered. Air static temperature was kept at 300 K. Location of baffles and jets along span-wise direction were represented as B1 to B4 and J1 to J3 and three lines along the stream-wise

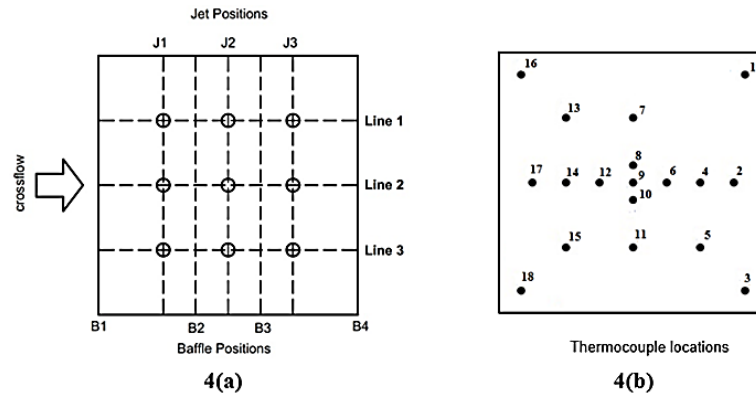


**Fig. 4. (a) Representative position of jet rows, baffles and stream-wise lines and (b) Position of thermocouples.**

direction as Lines 1, 2, 3 were illustrated in Fig. 4a. Position of thermocouples are shown in Fig. 4b.

Along the stream wise direction, Lines 1, 2 and 3 were considered as the focal points to represent the variations of Nusselt number and heat transfer. Commercial CFD solver ANSYS Fluent was used for numerical simulations. Second order discretization scheme was used for the pressure, continuity, momentum, energy, turbulence kinetic energy, and specific dissipation rate. For the pressure velocity coupling, standard coupled algorithm was adopted. SST  $k-\omega$  turbulence model was used for the present investigation, as it maintains a fair balance between computational time and accuracy. Steady state simulations were carried out till convergence of solution was attained. Appropriate grid size of the model was selected based on a grid independence test. A grid of 1.7724 million and 1.7749 million cells for configuration 1 and configuration 2 respectively was found to be computationally accurate and efficient.

#### 4. VALIDATION

The numerical predictions are validated against results obtained from experimental measurements and is shown in Fig. 5.

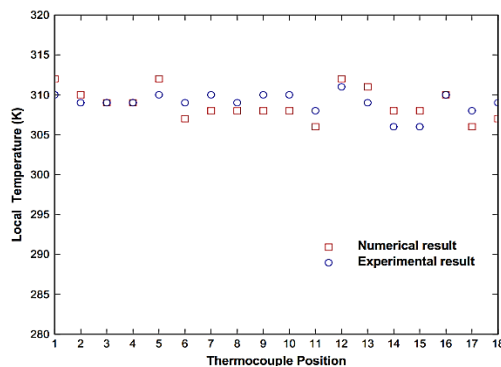


**Fig. 5. Validation of numerical values with experimental results.**

For a baffle clearance of 1 mm and a blow ratio of 0.75, experimentally determined temperatures were

compared with numerically predicted values at selected locations on the heated plate. It is found that experimental results are in good agreement with the numerical results with a maximum variation limited to  $\pm 2^\circ\text{C}$ .

#### 5. RESULTS

##### 5.1 Heat transfer results

Parametric effects of external cross-flow and baffle clearance on heat transfer characteristics were investigated for two baffle configurations. A comparison of surface averaged heat transfer coefficient with respect to blow ratio for various jet impingement configurations are shown in Fig. 6. Lower values of baffle clearance result in increased momentum and turbulence closer to the plate surface offering higher heat transfer coefficient. Presence of baffles creates regimes of flow reversal with high shearing rates.

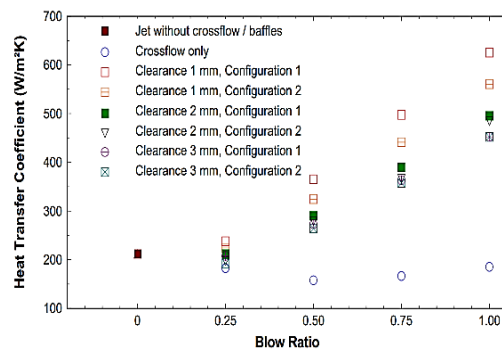


**Fig. 6. Computed surface averaged heat transfer coefficient for baffle configuration-1 and configuration-2 with various baffle clearances.**

It can also be observed that, at low blow ratio conditions, for a given clearance, baffle configuration does not play any significant role in heat transfer. However, at higher blow ratio, baffle configuration is a deciding factor of overall heat transfer as well as pressure drop. Baffle configuration-1, with minimum clearance results in

higher values of heat transfer compared to configuration-2. However, in either configuration, it can be established that, heat transfer is augmented by presence of baffles. This may be attributed to the comparatively loss of momentum of the flow downstream, caused by excessive turning encountered in configuration-2.

Figure 7 and 8 shows variation of Nusselt number along Line 2 and Line 1 respectively, along stream wise direction with representative location of jet and baffles for baffle configuration-2. It was observed that for all clearances, along the center line (Line 2), all Nusselt number curves coincide for 80% of stream-wise direction along the plate.

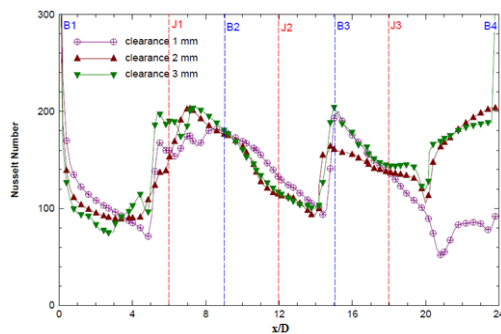


**Fig. 7. Variation of local Nusselt number along line 2.**

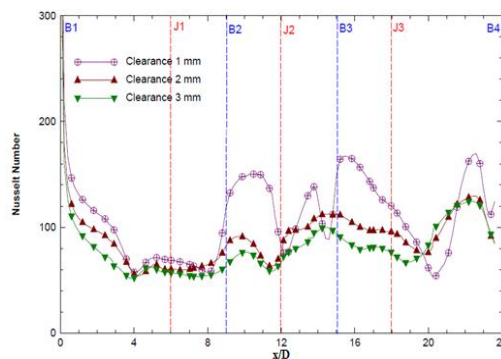


**Fig. 8. Variation of local Nusselt number along line 1.**

The interaction of external cross flow with first row of jets results in improvement of heat transfer as indicated by higher Nusselt number. Heat transfer augmentation by second and third rows of impinging jets are not significant compared to first row of jet. However, presence of baffles on stream-wise direction always tends to improve heat transfer significantly, represented by peaks of local Nusselt number, in the vicinity of baffles. Heat transfer coefficient contours of multiple jet system with baffle configuration-2 are illustrated in Fig. 9. The temperature field, the distribution of local Nusselt number, and the local friction coefficient are symmetrical about Line 2. It is noted that, local heat transfer coefficient reaches a maximum, just downstream of second row of baffles, at higher blow ratio and minimum clearance condition.

Figure 10 shows local Nusselt number distribution along Line 2 for different blow ratios for system configuration-2 with baffle clearance of 1 mm. It is observed that local Nusselt number is higher at higher blow ratio as expected. A general trend of local Nusselt number under various blow ratios considered shows similar pattern except in the region between first row of jet and second row of baffles. At lower blow ratio, ( $BR < 0.5$ ), the presence of second row of baffles diverts the cross-flow, and therefore, cross-flow contribution to heat transfer will be significantly reduced. However, at higher values of blow ratio, forced cross-flow velocities will be relatively higher beneath the second row of baffles which augments the heat transfer along with jet contribution from second row of jets. Therefore, it can be concluded that, although cross flow strength may significantly alter the flow patterns at local level, the line-averaged Nusselt number increases with increase in blow ratio.

## 5.2 Heat Transfer and Pressure Drop Comparison.

Figure 11 shows variation of dimensionless surface average Nusselt number with dimensionless average friction coefficient considering different baffle clearances. Here  $Nu/Nu_0$  is defined as a ratio of Nusselt number of baffled configuration to the Nusselt number of non-baffled configuration keeping same cross flow and jet conditions. This ratio indicates the enhancement in the Nusselt number by using baffles as compared to simple cross flow assisted jet impingement configuration. Similarly,  $ff_0$  is defined as a ratio of friction coefficient of baffled configuration to the friction coefficient of non-baffled configuration. For system with baffle clearance of 3mm, 100% increase in dimensionless Nusselt number is followed by 47% increase dimensionless friction coefficient, while 83% increase was observed for baffle clearance of 1 mm. Therefore, it could be inferred that, higher baffle clearance offers a better heat transfer with respect to pressure drop characteristics. However, relation between these Nusselt Number and friction coefficient with overall heat transfer and pressure drop is achieved through definition of thermo-hydraulic performance factor.

The thermo-hydraulic performance factor of a baffle assisted jet impingement system can be defined as

$$\phi = \frac{Nu/Nu_0}{\left(\frac{f}{f_0}\right)^{1/3}} \quad (1)$$

The thermo-hydraulic performance for jet impingement systems having baffle configuration-1 and configuration-2 operating under various clearances are shown in Fig. 12. From the graph obtained, it can be concluded that the performance factor is maximum in the case of configuration-2 and minimum for configuration-1 for any blow ratios. Any configuration offering performance factor near unity or above indicates optimal heat transfer and flow characteristics. However, in the

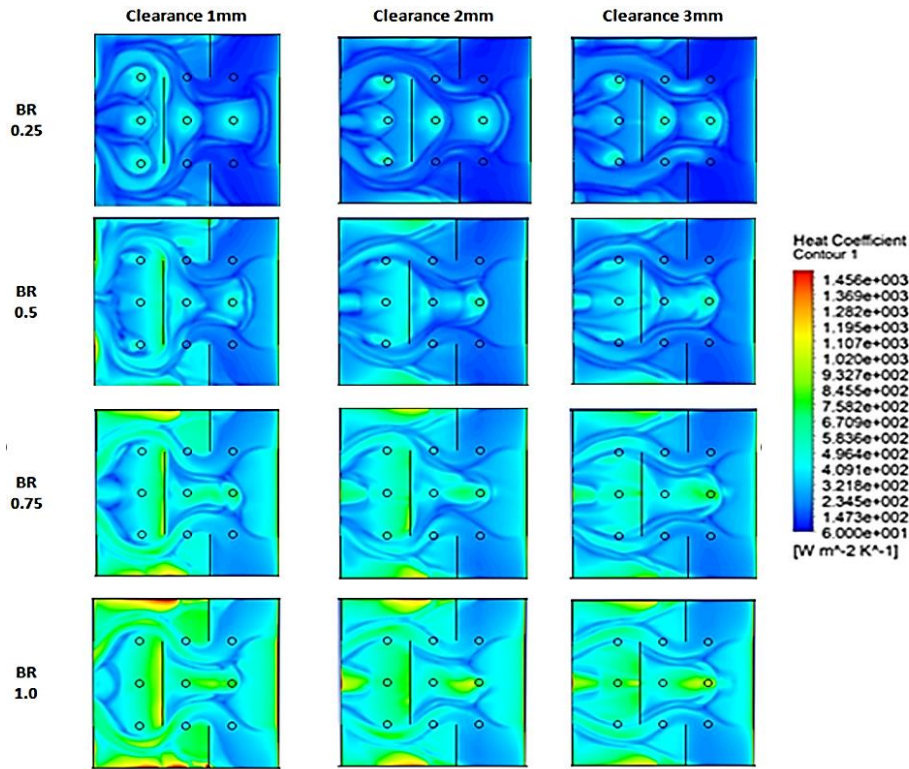


Fig. 9. Heat transfer coefficient contours of multiple jet system of baffle configuration-2 with clearance of 1 mm.

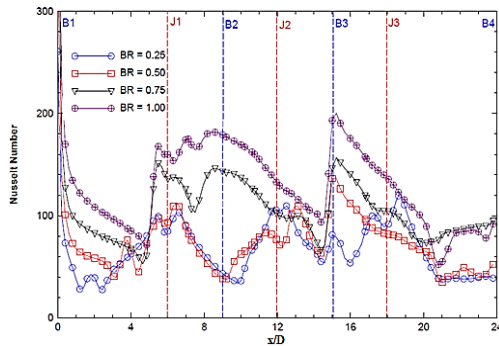


Fig. 10. Variation of local Nusselt number along Line 2 for different blow ratios.

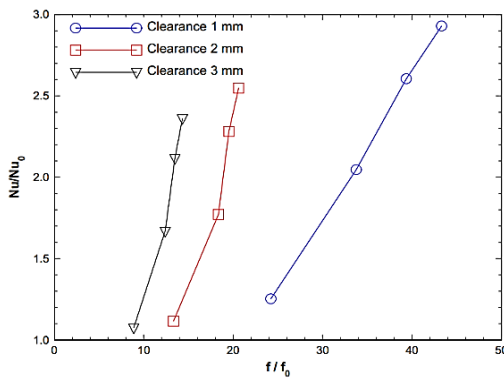


Fig. 11. Dimensionless Nusselt Number vs Friction coefficient.

case of jet impingement systems, performance factor alone cannot ensure absence of hot spots. Previous

discussions showed that higher heat transfer rates were achieved at lower clearance values, for which performance factor is quite low. However, considering pumping work of external cross flow and better heat transfer, optimal value of clearance may be sought. Thus, determination of optimum operating parameters such as blow ratio and baffle clearance which provide higher values of surface averaged Nusselt number while minimizing the friction coefficient constitutes an optimization problem for baffle assisted jet impingement system.

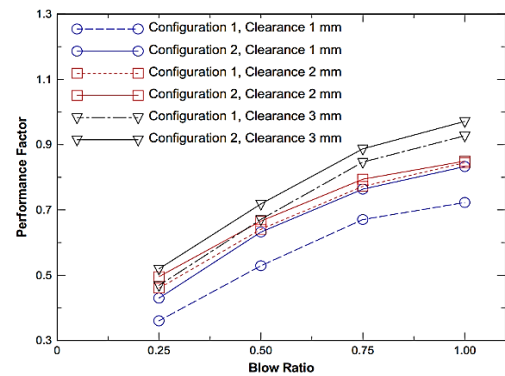


Fig. 12. Thermo-hydraulic performance factor for baffle configuration 1 and 2.

Optimization Study with Genetic Algorithm (GA) and Analysis by Artificial Neural Network (ANN).

In this work, cross flow velocity (decided by the blow ratio), baffle clearance, and height of channel,

represented by  $H/D$  ratio are taken as operating parameters. The two objectives are 1) maximize the average Nusselt number and 2) minimize the pressure drop. This results in a multi-objective optimization problem that can be solved by combining Genetic Algorithm (GA) with Artificial Neural Network (ANN) to provide optimal solutions with minimum computational effort.

The concept of Pareto optimality is used for solving this multi-objective optimization problem. In this concept, one design is considered to be dominating if it is better than all other designs in one objective and better or equal to other designs in other objectives. Present study employs the genetic algorithm (GA) as the optimization algorithm.

Creating a random population is the first step in this algorithm. The population consists of individuals which have encoded values called genes that can describe the individual. In this case, each individual design would have three genes and each gene represents the cross-flow velocity, height of the channel, and clearance respectively in their encoded form. For encoding the real values of design parameters into gene values, a linear mapping was utilized. All the parametric values were mapped into a range of 1-100 and hence the gene values will always have the same range of values. This helps to implement genetic operators that operate on all gene values irrespective of the actual value differences.

In the second stage, the average Nusselt number and pressure drop were calculated for each individual set of parameters. These objective function values are obtained from computational simulation results. Each simulation is computationally expensive in time and resources even on a high-end processor. Hence a generation of 30 individual sets might take several days to complete. Iterating over such generations would result in huge computational effort. To prevent this, Response Surface Methodology (RSM) was used to replace simulations.

Once the evaluation is done, the parents were selected from the current generation based on their fitness values. These parents are then used to produce new offspring for the next generation through crossover and mutation operations. The crossover operation mates two parents to produce two new offspring. The process continues till a specified convergence criterion is satisfied. In this work, 100 generations were run even if no change in the objective function was observed after approximately 40 generations. Figure 13 shows the variation of Nusselt number with generation. It can be seen that the Nusselt number has improved considerably from the initial generation and later, no improvement was observed beyond the 40<sup>th</sup> generation.

This multi-objective optimization results in non-dominated designs known as Pareto Front. The Pareto front obtained after the optimization run is shown in Fig. 14. Each and every point on this line is an optimal solution. For example, a design point on the Pareto front that provides a Nusselt number of 120, no other design from a feasible set can provide

a Nusselt number greater than 120, without degrading the pressure drop. The choice can be made based on whether priority needs to be given for a higher Nusselt number or lower Pressure drop.

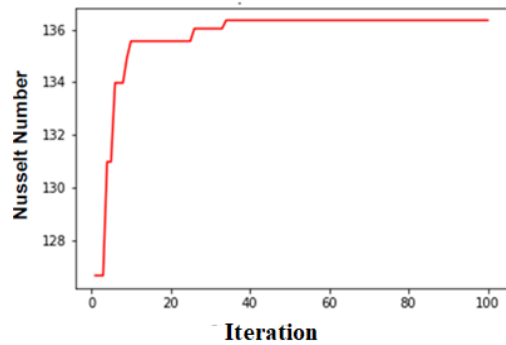


**Fig. 13. Nusselt number improvement with GA iteration.**

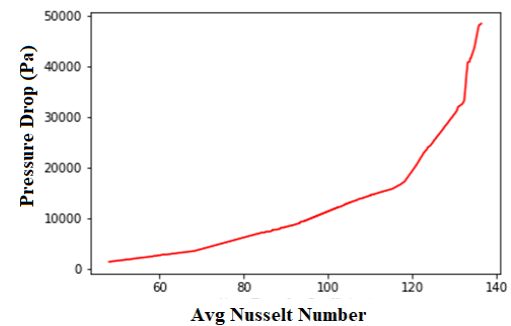


**Fig. 14. Pareto Front from GA optimization.**

An Artificial Neural Network (ANN) model based on Response Surface Methodology (RSM) was incorporated in the genetic algorithm code to evaluate the objective functions. While a numerical simulation takes a few hours, a trained ANN predicts the function values instantaneously. This method involves generating designs that fill the design space uniformly. Total 32 designs were created for training. Numerical simulations were carried out to calculate the Nusselt number and pressure drop for each of these designs. This data is then used to train the ANN. The resulting ANN consisted of 4 hidden layers and each consisting of 6, 12, 12 and 6 neurons respectively. The code was created in Python using the libraries TensorFlow and Keras. Using this method, the predicted Nusselt number and pressure drop are plotted against actual values of Nusselt number and pressure drop respectively on Figs. 15 and 16. Points lying on a 45<sup>o</sup> line would imply a perfect match. In both figures, it was observed that the predicted values are in close agreement with the actual values from the simulation. Therefore, the ANN results are validated which can replace simulations in GA optimization techniques. Average heat transfer coefficient can be expressed in terms of operating

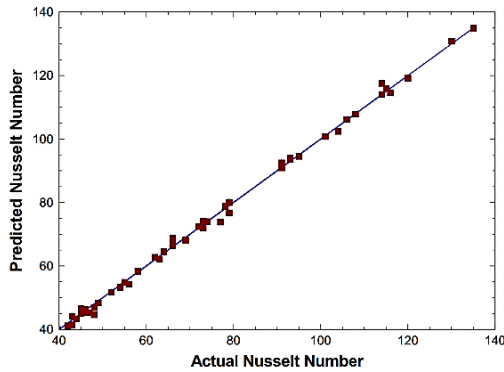


**Fig. 15. Comparison of ANN results with CFD results in terms of average Nusselt number.**

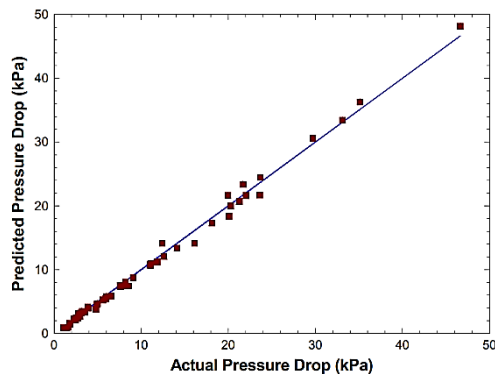


**Fig.16. Comparison of ANN results with CFD results in terms of average pressure drop.**

parameters for jet impingement systems with baffle configuration-2 using a linear regression model. Based on 44 data points obtained from simulations, an equation for surface averaged heat transfer coefficient can be obtained with an average of  $\pm 4.25\%$  error as given below.

$$h = 12.77V_c + 9.607H - 35.66C + 15.24 \quad (2)$$

Equation (2) when applied to baffle configuration-1, yields an average heat transfer coefficient with an average error of  $\pm 13.42\%$  based on 44 data points.

Therefore, Eq. (2) provides a better estimate for surface averaged heat transfer coefficient of cross flow aided multiple jet impingement system with baffle configuration-2.

## 6. CONCLUSIONS

CFD analysis of a baffle-assisted multi-jet impingement of air on a heated plate subjected to constant heat flux and cross-flow has been carried out. A set of half-span baffles were introduced across flow direction with two types of configurations (segmented and split) and their heat transfer and pressure drop characteristics were determined. The effects of baffle clearance, cross-flow, and  $H/D$  ratio were studied in detail and optimal operating parameters were identified with the aid of Genetic

algorithm and Artificial Neural Network and the following conclusions were made:

1. Baffle-assisted jet impingement system offers superior heat transfer performance for all blow ratios. The configuration-1 provides better heat transfer compared to configuration-2 at high blow ratios. However, considering the thermo-hydraulic performance factor, baffle configuration-2 gives better heat transfer benefits for a given cross-flow pressure drop.

2. Lowering baffle clearance results in an increase of Nusselt number. However, the pressure drop encountered will be quite large. In the present analysis, jet impingement system with baffle clearance of 3 mm and configuration-2 is found to be the best design to achieve a balance between heat transfer and pressure drop that offers a performance factor near unity.

3. Optimal solutions of heat transfer and pressure drop were evaluated for the present multi-objective optimization problem using a Genetic Algorithm (GA) for baffle configuration-2. A design point on the Pareto front can be chosen for a desired value of heat transfer or pressure drop, which will be one of the optimal values available for the system.

4. Artificial Neural Network (ANN) based solutions can replace time-consuming CFD simulations, to predict optimal solutions. Comparison between CFD simulation results and ANN predictions strongly agree with each other.

5. A linear regression model equation for surface averaged heat transfer coefficient has been developed, which can predict the heat transfer coefficient with an average error of  $\pm 4.25\%$  for configuration-2 and  $\pm 13.42\%$  for configuration-1.

## REFERENCES

- Angioletti, M., R. M. Di Tommaso, E. Nino and G. Ruocco (2003). Simultaneous visualization of flow field and evaluation of local heat transfer by transitional impinging jets. *Int. J. Heat and Mass Transfer* 46, 1703-1713.
- Berner, C., F. Durst and D. M. McEligot (1984). Flow Around Baffles. *ASME journal of heat transfer* 106, 743-749.
- Chance, J. L. (1974). Experimental investigation of air impingement heat transfer under an array of round jets. *TAPPI* 57 (6), 108-112.
- Chandramohan, P., S. N. Murugesan and S. Arivazhagan (2017). Heat Transfer Analysis of Flat Plate Subjected to Multi-Jet Air Impingement using Principal Component Analysis and Computational Technique. *Journal of Applied Fluid Mechanics* 10 (1), 293-306.
- Chandramohan, P., S. N. Murugesan and S. Arivazhagan (2021). Experimental Investigation of Multi-Jet Air Impingement in Various Conditions and Analysis using Desirability Based Response Surface

- Methodology. *Journal of Applied Fluid Mechanics* 14 (1), 131-145.
- Chen, M., R. Chalupa, A.C. West and V. Modi (2000). High schmidt mass transfer in a laminar impinging slot jet flow. *Int. J. Heat Mass Transfer* 43, 3907– 3915.
- Craft, T. J., B. E. Launder and K. Suga (1996). Development and application of a cubic eddy-viscosity model of turbulence. *Int. J. Heat and Fluid Flow* 17, 108-115.
- Dhanasegaran, R. and S. Pugazhendhi (2017). Computational Study of Flow and Heat Transfer with Anti Cross-Flows (ACF) Jet Impingement Cooling For Different Heights of Corrugate, *Proceedings of the ASME 2017 Transfer Summer Conference HT2017 July 9-12, 2017, Washington, USA, HT2017-4783*,
- Dutta, S., P. Dutta, R. E. Jones and J. A. Khan (1997). Experimental Study of Heat Transfer Coefficient Enhancement with Inclined Solid and Perforated Baffles, *International Mechanical Engineering Congress and Exposition, Dallas, Texas, ASME Paper No. 97- WA/HT-4*.
- Florschuetz, L. W., C. R. Truman and D. E. Metzger (1981). Stream-wise flow and heat transfer distributions for jet array impingement with cross-flow. *ASME Trans. J. Heat Transfer* 103, 337-342.
- Habib, M. A., A. M. Mobarak, A.M. Attya and A. Z. Aly (1992). An experimental investigation of heat-transfer and flow in channels with stream-wise-periodic flow. *Energy* 17(11), 1049-1058.
- Illyas, S. M., B. R. R. Bapu and V. V. S. Rao (2019). Experimental Analysis of Heat Transfer and Multi-Objective Optimization of Swirling Jet Impingement on a Flat Surface. *Journal of Applied Fluid Mechanics* 12 (3), 803-817.
- Jambunathan, K., E. Lai, M. Moss and B. Button (1992). A review of heat transfer data for single circular jet impingement. *Int. J. Heat Fluid Flow* 13, 106–115.
- Kline, S. J. and F. A. McClintock (1953). Describing uncertainties in single-sample experiments. *Mechanical Engineering* 75(1), 3–8.
- Lou, Z., A. Mujumdar, C. and Yap (2005). Effects of geometric parameters on confined impinging jet heat transfer. *Appl. Therm. Engineering* 25, 2687–2697.
- Masip, Y., A. Rivas, G.S. Larraona, R. Antón, J.C. Ramos and B. Moshfegh (2012). Experimental study of the turbulent flow around a single wall-mounted cube exposed to a cross-flow and an impinging jet, *International Journal of Heat and Fluid Flow* 38, 50-71.
- Metzger, D. E., L. W. Florschuetz, D. I. Takeuchi, R.D. Behee and R.A. Berry (1979). Heat transfer characteristics for inline and staggered arrays of circular jets with cross-flow of spent air. *ASME Trans. J. Heat Transfer* 101, 526-531.
- Metzger, D. E. and R. Korstad (1972). Effects of cross-flow on impingement heat transfer, *ASME Trans. J. Eng. Power* 94, 35-41.
- Mohamed, M. M. (2006). Air cooling characteristics of a uniform square modules array for electronic device heat sink. *Applied Thermal Engineering* 26, 486-493.
- Nasiruddin, M. H., Kamran, and Siddiqui (2007). Heat transfer augmentation in a heat exchanger tube using a baffle. *Int. J. of Heat and Fluid Flow* 28, 318–328.
- Obot, N. T. and T. A. Trabold (1987). Impingement heat transfer within arrays of circularjets: part 1-effects of minimum, intermediate, and complete cross-flow for small and large spacing. *ASME Trans. J. Heat Transfer* 109, 872-879.
- Popovac, M. and K. Hanjalic (2007). Large-eddy simulations of flow over a jet impinged wall mounted cube in a cross stream, *International Journal of Heat and Fluid Flow* 28, 1360-1378.
- Popovac, M. and K. Hanjalic (2009). Vortices and heat flux around a wall-mounted cube cooled simultaneously by a jet and a cross-flow. *International Journal of Heat and Mass Transfer* 52, 4047-4062.
- Rundström, D. and B. Moshfegh (2006). Investigation of flow and heat transfer of an impinging jet in a cross-flow for cooling of a heated cube. *ASME Journal of Electronic Packaging* 128, 150-156.
- Rundström, D. and B. Moshfegh (2008). Investigation of heat transfer and pressure drop of an impinging jet in a cross-flow for cooling of a heated cube. *ASME Journal of Heat Transfer* 130, 121401.
- Shukla, A. K. and A. Dewan (2017), Convective Heat Transfer Enhancement using Slot Jet Impingement on a Detached Rib Surface, *Journal of Applied Fluid Mechanics* 10 (6), 1615-1627.
- Tummers, M. J., M. A. Flikweert, K. Hanjalic, R. Rodink, and B. Moshfegh (2005). Impinging jet cooling of wall mounted cubes, in: W. Rodi (Ed.), *Engineering Turbulence Modeling and Experiments* 6, Elsevier Ltd., Cambridge, UK. 773-782.
- Van Heiningen, A., A. Mujumdar and W. Douglas (1976). Numerical prediction of the flow field and impingement heat transfer caused by a laminar slot jet. *J. Heat Transfer* 98, 654–658.
- Wang, T., M. Lin, and R. S. Bunker (2005). Flow and heat transfer of confined impingement jets cooling using a 3-D transient liquid crystal scheme, *Int. J. Heat Mass Transfer* 48 (23–24)

4887–4903.

- Yemenici, O., Z. A. Firatoglu and H. Umur (2012). An experimental investigation of flow and heat transfer characteristics over blocked surfaces in laminar and turbulent flows. *International Journal of Heat and Mass Transfer* 55, 3641-3649.
- Yu, Rao., Peng, Chen., Chaoyi, and Wan. (2016). Experimental and numerical investigation of

impingement heat transfer on the surface with micro W-shaped ribs. *Int. J. of Heat and Mass Transfer* 93, 683-694.

- Zuckerman, N. and N. Lior (2006). Jet impingement heat transfer: physics, correlations, and numerical modeling. *Adv. Heat Transfer* 39, 565–631.